

# Optical circular polarization induced by axion-like particles in blazars

Run-Min Yao,<sup>1,2,\*</sup> Xiao-Jun Bi,<sup>1,2,†</sup> Jin-Wei Wang,<sup>3,4,5,6,‡</sup> and Peng-Fei Yin<sup>1,§</sup>

<sup>1</sup>Key Laboratory of Particle Astrophysics, Institute of High Energy Physics, Chinese Academy of Sciences, Beijing, China

<sup>2</sup>School of Physical Sciences, University of Chinese Academy of Sciences, Beijing, China

<sup>3</sup>Tsung-Dao Lee Institute and School of Physics and Astronomy,

Shanghai Jiao Tong University, 800 Dongchuan Road, Shanghai 200240, China

<sup>4</sup>Scuola Internazionale Superiore di Studi Avanzati (SISSA), via Bonomea 265, 34136 Trieste, Italy

<sup>5</sup>INFN, Sezione di Trieste, via Valerio 2, 34127 Trieste, Italy

<sup>6</sup>Institute for Fundamental Physics of the Universe (IFPU), via Beirut 2, 34151 Trieste, Italy

(Dated: September 29, 2022)

We propose that the interaction between the axion-like particles (ALPs) and photons can be a possible origin of the optical circular polarization (CP) in blazars. The non-detection of the optical CP at the level of 0.1% can be used to place a constraint on the ALP-photon coupling  $g_{a\gamma} \cdot B_{T0} \lesssim 7.9 \times 10^{-12} \text{ G} \cdot \text{GeV}^{-1}$  for  $m_a \lesssim 10^{-13} \text{ eV}$ , which depends on the magnetic field model of the blazar jet. This constraint would be stringent for the blazar models with a large magnetic field strength, such as hadronic radiation models. We also perform an analysis for the possible observations of the optical CP in two blazars, and find that they could be explained by the ALP-photon coupling of  $\mathcal{O}(10^{-12}) \text{ GeV}^{-1}$ . As an outlook, our analysis can be improved by further researches on the radiation models of blazars and high-precision simultaneous measurements of the optical linear polarization and CP.

## I. INTRODUCTION

Axion-like particles (ALPs) are very light pseudo-scalar particles that appear in many extensions of the Standard Model (SM) [1–7]. These particles constitute a generalization of the quantum chromodynamics (QCD) axion, which is a pseudo-Goldstone boson arising from the Peccei-Quinn symmetry breaking mechanism and can be treated as an excellent solution to the strong  $CP$  problem [8–12]. Meanwhile, unlike the QCD axion, the coupling and mass of the ALP are, in principle, independent parameters, thus a much wider parameter space is spanned in the ALP scenario. ALPs are extremely appealing as they can also play an important role in cosmology and astrophysics [13–16]. For instance, ALPs are good candidates for the cold dark matter [17].

At low energies, ALPs could interact with the SM particles through the effective operators that are suppressed by some high energy scales [18]. For example, ALPs may interact with the electromagnetic sector through the Lagrangian term  $\mathcal{L} = g_{a\gamma} a \mathbf{E} \cdot \mathbf{B}$ . This interaction can lead to two distinct effects in astrophysics, which provide promising ways to detect ALPs. One is the polarization rotation of photons as they propagate in a variable ALP background field, due to the change of the dispersion relation of the photon [19–24]. The other is the ALP-photon conversion in the external magnetic field [25, 26]. The mixing occurs between the ALPs and the photon polarization component that in parallel to the magnetic field. In particular, this process changes not only the amplitude

but also polarization of the photon [26, 27]. Considering that the ALP-photon coupling is particularly weak, many studies focus on the conversion for high energy photons [28–36] or the resonant conversion in strong magnetic fields [37–46]. Otherwise, the magnetic fields in large scales, e.g., the supercluster at scale of  $\sim 10 \text{ Mpc}$ , are needed to achieve a significant conversion [47–49].

Many studies have addressed the ALP effects on the observed spectrum and polarization state of  $\gamma$ -ray from sources like blazars in astrophysical magnetic fields [28–36, 50–56], including those in the blazar jet, galaxy cluster, intergalactic space, and Milky Way. However, the mixing effect is rarely discussed for low energy photons, especially within the source region of blazars. In fact, there are some advantages to study such effect. It is easier to measure the polarization of low energy photons with high precision [57, 58]. Besides, with the multi-wavelength observations of blazars, we have a better understanding of their properties, such as the radiation mechanism and the magnetic field structures [59, 60], which in turn helps us to understand the initial polarization state of photons. Based on these facts, it is an intriguing project to investigate the ALP effect on the optical photon polarization state from blazars.

It is expected that ALPs would not significantly change the flux and linear polarization (LP) of the optical photons from blazars. However, we find that under some suitable conditions, ultra-light ALPs can lead to an appreciable circular polarization (CP), which may be an origin of the optical CP in blazars. Conversely, the ALPs can be explored through the possible CP measurements of blazars.

In recent years, several optical polarization monitoring programs have been carried out, and mainly focus on the linear polarization (LP) signature [61]. However, the optical circular polarization in blazars has rarely been

\* yaorunmin@ihep.ac.cn

† bixj@ihep.ac.cn

‡ jinwei.wang@sissa.it

§ yinpf@ihep.ac.cn

measured. This is partly because that the optical CP is expected to be low in usual physical processes [62], requiring very sensitive instruments to deliver CP measurements. If the ALP-photon mixing can lead to an appreciable CP on the optical photons from blazars, we appeal to implement more sensitive experiments that can simultaneously measure the optical LP and CP to further nail down the effects of ALPs.

The paper is organized as follows. In Sec. II, we present a brief calculation routine of the ALP-photon mixing and derive the CP formulas under the weak-mixing condition. In Sec. III, we introduce the jet configuration of BL Lacs and obtain results using the CP formulas. In Sec. IV, we analyze the ALP effects in the possible CP observations of two blazars. In Sec. V, we discuss several relevant factors that may affect the results. Conclusions are given in Sec. VI. Note that all equations are expressed in Lorentz–Heaviside units throughout the paper.

## II. ALP-PHOTON MIXING IN MAGNETIC FIELDS

### A. Mixing in one domain

The calculation routines used for the ALP-photon conversion have been detailed described in many papers [33–35, 50]. Nevertheless, for the reader's convenience, we briefly summarize all necessary elements here. The ALP-photon system can be described by the Lagrangian

$$\begin{aligned}\mathcal{L}_{\text{ALP}} &= \frac{1}{2}\partial^\mu a \partial_\mu a - \frac{1}{2}m_a^2 a^2 - \frac{1}{4}g_{a\gamma} a F_{\mu\nu} \tilde{F}^{\mu\nu} \\ &= \frac{1}{2}\partial^\mu a \partial_\mu a - \frac{1}{2}m_a^2 a^2 + g_{a\gamma} a \mathbf{E} \cdot \mathbf{B},\end{aligned}\quad (1)$$

where  $a$  denotes the ALP field,  $F_{\mu\nu}$  and  $\tilde{F}^{\mu\nu}$  are the electromagnetic tensor and its dual, respectively. For the ALP, the mass  $m_a$  is unrelated to the coupling  $g_{a\gamma}$ . The ALP-photon mixing in the presence of an external magnetic field  $\mathbf{B}$  is characterized by the  $a\gamma\gamma$  vertex in the Lagrangian. Only the transverse component of the external magnetic field  $\mathbf{B}_T$  with respect to the direction of beam propagation matters.

We assume a monochromatic ALP-photon beam with energy of  $E \gg m_a$  propagating in the  $z$  direction. In the short-wavelength approximation, the equation of motion (EOM) can be written as [26]

$$\left(i \frac{d}{dz} + E + \mathcal{M}\right) \psi(z) = 0 \quad (2)$$

with

$$\psi(z) = \begin{pmatrix} A_x(z) \\ A_y(z) \\ a(z) \end{pmatrix}, \quad (3)$$

where  $A_x(z)$  and  $A_y(z)$  denote the LP amplitudes of the photon along the  $x$ - and  $y$ -axis, respectively, and  $a(z)$  is the ALP amplitude.

The magnetic field is often supposed to be homogeneous in a single small domain. If its transverse component  $\mathbf{B}_T$  is set along with the  $y$ -axis, the mixing matrix is given by [63]

$$\mathcal{M}^{(0)} = \begin{pmatrix} \Delta_\perp & 0 & 0 \\ 0 & \Delta_\parallel & \Delta_{a\gamma} \\ 0 & \Delta_{a\gamma} & \Delta_a \end{pmatrix}, \quad (4)$$

with

$$\Delta_{a\gamma} \equiv \frac{1}{2} g_{a\gamma} B_T, \quad (5)$$

$$\Delta_a \equiv -\frac{m_a^2}{2E}. \quad (6)$$

$\Delta_{a\gamma}$  and  $\Delta_a$  account for the ALP-photon mixing and ALP mass effect, respectively. Since we consider photon in the optical band here, other off-diagonal  $\Delta$ -terms related to the Faraday rotation are neglected.

The diagonal terms related to the photon constitute four parts as [64, 65]

$$\Delta_\perp \equiv \Delta_{\text{pl}} + \Delta_{\text{abs}} + \Delta_{\text{CMB}} + 2\Delta_{\text{QED}}, \quad (7)$$

$$\Delta_\parallel \equiv \Delta_{\text{pl}} + \Delta_{\text{abs}} + \Delta_{\text{CMB}} + 3.5\Delta_{\text{QED}}, \quad (8)$$

with

$$\Delta_{\text{pl}} \equiv -\frac{\omega_{\text{pl}}^2}{2E}, \quad (9)$$

$$\Delta_{\text{abs}} \equiv \frac{i}{2\lambda_\gamma}, \quad (10)$$

$$\Delta_{\text{CMB}} \equiv \chi_{\text{CMB}} E, \quad (11)$$

$$\Delta_{\text{QED}} \equiv \frac{\alpha E}{45\pi} \left(\frac{B_T}{B_{\text{cr}}}\right)^2. \quad (12)$$

$\Delta_{\text{pl}}$  accounts for the effective photon mass when the beam propagates in the plasma with the frequency parameter  $\omega_{\text{pl}} = (4\pi\alpha n_e/m_e)^{1/2}$ , where  $\alpha$  is the fine-structure constant,  $n_e$  and  $m_e$  denote the electron number density and the electron mass, respectively. The other three contributions, including  $\Delta_{\text{abs}}$  the photon absorption term with the mean free path  $\lambda_\gamma$ ,  $\Delta_{\text{CMB}}$  the photon dispersion term induced by the cosmic microwave background with the refractive index  $\chi_{\text{CMB}} \simeq 0.522 \times 10^{-42}$  [66], and  $\Delta_{\text{QED}}$  the QED vacuum polarization term with  $B_{\text{cr}} \simeq 4.4 \times 10^{13}$  G, are negligible in the scenario here. That is to say, we can safely make the approximation  $\Delta_\parallel \approx \Delta_\perp \approx \Delta_{\text{pl}}$ .

In a general situation,  $\mathbf{B}_T$  is not along with but forms an angle  $\phi$  with the  $y$ -axis. Correspondingly, the mixing matrix can be obtained using the similarity transformation

$$\mathcal{M} = V^\dagger(\phi) \mathcal{M}^{(0)} V(\phi) \quad (13)$$

operated by the rotation matrix in the  $x$ - $y$  plane, namely

$$V(\phi) = \begin{pmatrix} \cos \phi & -\sin \phi & 0 \\ \sin \phi & \cos \phi & 0 \\ 0 & 0 & 1 \end{pmatrix}. \quad (14)$$

In view of our subsequent discussion, the polarization density matrix is introduced as

$$\rho(z) = \begin{pmatrix} A_x(z) \\ A_y(z) \\ a(z) \end{pmatrix} \otimes (A_x(z) \ A_y(z) \ a(z))^*, \quad (15)$$

which obeys the Liouville-Von Neumann equation

$$i \frac{d\rho}{dz} = [\rho, \mathcal{M}]. \quad (16)$$

The solution of Eq. (16) is

$$\rho(z) = \mathcal{T}(z, z_0) \rho(z_0) \mathcal{T}^\dagger(z, z_0), \quad (17)$$

where the transfer function  $\mathcal{T}(z, z_0)$  is the solution of the EOM in the form of  $\psi(z) = \mathcal{T}(z, z_0)\psi(z_0)$  with the initial condition  $\mathcal{T}(z_0, z_0) = 1$ . The probability that a photon/ALP beam initially in the state  $\rho(z_0)$  converts into the state  $\rho_f$  at a position with  $z$  can be computed as

$$P = \text{Tr}(\rho_f \mathcal{T}(z, z_0) \rho(z_0) \mathcal{T}^\dagger(z, z_0)). \quad (18)$$

For a fixed magnetic field, the probability that a photon polarized along the y-axis oscillates into an ALP after a distance  $d$  can simply read

$$P_{\gamma \rightarrow a} = \cos^2 \phi \sin^2(2\theta) \sin^2\left(\frac{\Delta_{\text{osc}} d}{2}\right), \quad (19)$$

with the ALP-photon mixing angle

$$\theta = \frac{1}{2} \arctan\left(\frac{2\Delta_{a\gamma}}{\Delta_{\parallel} - \Delta_a}\right) \quad (20)$$

and the oscillation wave number

$$\Delta_{\text{osc}} = [(\Delta_a - \Delta_{\parallel})^2 + 4\Delta_{a\gamma}^2]^{1/2}. \quad (21)$$

In numerical calculation with a realistic configuration of the astrophysical magnetic field, the field environment can be sliced into  $N$  consecutive domains with homogeneous magnetic fields, within which the EOM is solved exactly with different physical parameters, continuously renewing the polarization density matrix along the beam propagation.

## B. Optical circular polarization

The  $2 \times 2$  density matrix of the photon polarization (i.e., the 2-2 block of the density matrix for the ALP-photon system) can be expressed in terms of the Stokes parameters [67]

$$\rho_\gamma = \frac{1}{2} \begin{pmatrix} I + Q & U - iV \\ U + iV & I - Q \end{pmatrix}. \quad (22)$$

The degree of CP  $\Pi_C$  is defined as [68]

$$\Pi_C \equiv \frac{V}{I}. \quad (23)$$

In this study, we work within the weak-mixing condition

$$\begin{aligned} |\Delta_{\text{pl}}| &\gg \Delta_{a\gamma}, \\ |\Delta_{\text{pl}}| &\gg \Delta_a. \end{aligned} \quad (24)$$

In this regime,  $\theta \ll 1$  and the conversion probability turns out to be vanishingly small. Expanding Eq. (17) and neglecting the high order terms, the evolution of the Stokes parameters in a single domain region can be obtained as

$$I(z) = I(z_0) - \mathcal{I}(1 - \cos \kappa), \quad (25)$$

$$Q(z) = Q(z_0) - \mathcal{Q}_1(1 - \cos \kappa) - \mathcal{Q}_2 \sin \kappa, \quad (26)$$

$$U(z) = U(z_0) - \mathcal{U}_1(1 - \cos \kappa) - \mathcal{U}_2 \sin \kappa, \quad (27)$$

$$V(z) = V(z_0) \cos \kappa + \mathcal{V} \sin \kappa, \quad (28)$$

where

$$\mathcal{I} \equiv Q(z_0) \sin^2 2\phi, \quad (29)$$

$$\mathcal{Q}_1 \equiv \frac{1}{2} U(z_0) \sin 4\phi, \quad (30)$$

$$\mathcal{Q}_2 \equiv V(z_0) \sin 2\phi, \quad (31)$$

$$\mathcal{U}_1 \equiv [Q(z_0) \sin 2\phi + U(z_0) \cos 2\phi] \cos 2\phi, \quad (32)$$

$$\mathcal{U}_2 \equiv V(z_0) \cos 2\phi, \quad (33)$$

$$\mathcal{V} \equiv Q(z_0) \sin 2\phi + U(z_0) \cos 2\phi, \quad (34)$$

$$\kappa \equiv \left( \frac{\Delta_{a\gamma}^2}{\Delta_{\text{pl}}} - \frac{1}{2} \Delta_a \right) (z - z_0). \quad (35)$$

Supposing  $|\kappa| \ll 1$  in each domain and the degree of CP of the incident beam can be neglected, the above equations show that the change of  $I$ ,  $Q$ ,  $U$  is negligible at first leading order. For the CP, we can evaluate it across multi domains as

$$\begin{aligned} &V(z) - V(z_0) \\ &\approx \int_{z_0}^z \mathcal{V} \left( \frac{\Delta_{a\gamma}^2}{\Delta_{\text{pl}}} - \frac{1}{2} \Delta_a \right) dz' \\ &= - \frac{m_e g_{a\gamma}^2 \mathcal{V} E}{8\pi\alpha} \int_{z_0}^z \frac{B_T^2(z')}{n_e(z')} dz' + \frac{m_a^2}{4E} \mathcal{V} (z - z_0). \end{aligned} \quad (36)$$

The parameter  $\mathcal{V}$  is determined by the LP state of incident photons and the direction of the transverse magnetic field. For the above equation, we have made the assumption that the direction of transverse magnetic field remains unchanged, thus  $\mathcal{V}$  can be treated as constant. A general polarization density matrix of a beam of linearly polarized photons can be written as

$$\rho_\gamma(\Pi_L, \psi) = \begin{pmatrix} \frac{1 - \Pi_L \cos 2\psi}{2} & \frac{\Pi_L \sin 2\psi}{2} \\ \frac{\Pi_L \sin 2\psi}{2} & \frac{1 + \Pi_L \cos 2\psi}{2} \end{pmatrix}, \quad (37)$$

$$\Pi_L \equiv \frac{\sqrt{Q^2 + U^2}}{I},$$

where  $\Pi_L$  is the degree of LP and  $\psi$  is the polarization angle relative to the y-axis. Then, Eq. (34) can be rewritten as

$$\mathcal{V} = \Pi_L \sin 2(\phi - \psi). \quad (38)$$

The above equations show that the magnitude of the ALP induced CP is proportional to the LP degree of the photon in the weak-mixing regime. When  $\phi - \psi$ , which denotes the angle between the LP and the transverse magnetic field, equals  $(2k + 1)\pi/4$  with  $k \in \mathbb{Z}$ ,  $\mathcal{V}$  reaches the extreme value  $\pm\Pi_L$ .

Even though the energy of the photon and the magnetic field may not be high, the integration indicates that the ALPs can induce a considerable CP as long as the field environment is suitable and the spatial scale of magnetic field is large enough. This makes blazar a good candidate source as discussed in the next section.

### III. APPLICATION IN BLAZARS

*Blazars* are active galactic nuclei with a relativistic jet pointing very close to earth [59]. The highly collimated and Doppler boosted jet make them bright and variable in all wavebands from the radio to  $\gamma$ -ray [60]. Blazars are categorized as BL Lac objects (BL Lacs) [69] and flat-spectrum radio quasars (FSRQs) [70], which were mostly called optically violent variable quasars. Compared to BL Lacs, FSRQs are generally more luminous and show broad emission lines in the optical and UV bands. The jet of blazar can reach kpc and composes of a relatively constructed magnetic field.

The CP in the optical emissions is hardly detected in Blazars, while the degree of LP is typically at a level of  $\sim 10\%$  and can be up to  $\sim 50\%$  sometimes [61, 71]. Therefore, we can set constraint on the parameters of the ALP utilizing the effect discussed in the previous section. We focus on BL Lacs in the discussion below, considering that the field environment of FSRQs are more complicated and the geometry and intensity of  $\mathbf{B}$  are less clear compared to BL Lacs [72, 73].

#### A. Field configuration of BL Lacs

Faraday rotation measure (RM) is an important tool in astronomy, and enables one to study the magnetic field and the electron number density of blazar jets. Many observations have detected the transverse RM gradients across the jets of BL Lacs, which evidence that these jets have the toroidal or helical magnetic fields [74–76]. Based on some simple conservation laws, the conservation of the Poynting flux demands that the magnetic field strength varies as  $d^{-1}$ , where  $d$  is the transverse size of the jet [77, 78]. The conservation of particles demands that their density vary as  $r^{-2}$  [79], where  $r$  is the distance from the start of the jet. Hence, we adopt the conical shaped model used in [50, 51] here. In the co-moving frame, the transverse magnetic field and electron density of the jet

are modelled by following,

$$B_T^{\text{jet}} = B_{T0} \left( \frac{r}{r_E} \right)^{-1} \quad (39)$$

$$n_e^{\text{jet}} = n_{e0} \left( \frac{r}{r_E} \right)^{-2}, \quad (40)$$

for  $r > r_E$  with  $r_E$  the distance of the emission site to the central black hole. The value of  $r_E$  is usually inferred from the size of the emission region and the jet aperture angle, typically ranging from 0.01 pc to 0.1 pc [80]. It will be found in the latter discussion that the value of  $r_E$  has little effect on our results, thus we choose  $r_E = 0.05$  pc in order to be definite. Besides, the electron density at the emission site and the size of the jet are taken to be the typical values of  $n_{e0} \simeq 5 \times 10^4 \text{ cm}^{-3}$  and  $r_{\text{max}} \simeq 1 \text{ kpc}$  as [50, 51], respectively.

The spectral energy distributions (SEDs) of blazars are dominated by two distinct radiative components: a broad low-frequency component from radio to optical/UV or X-ray and a high-frequency component from X-ray to  $\gamma$ -ray. It is generally accepted that the low-frequency component is produced by the synchrotron radiation of relativistic electrons in the jets. For the interpretation of the high-frequency component, synchrotron self-Compton (SSC) or external Compton (EC) are the two main mechanisms. Hence, the popular models differ by the radiation particles into two kinds, namely leptonic (emission dominated by electrons and possibly positrons) and hadronic (emission dominated by protons) models [73, 81]. In the leptonic models, the SED fitting usually gives a magnetic field strength of 0.1 – 1 G for Intermediate BL Lacs and 1 – 3 G for Low-Frequency-Peaked BL Lacs [82]. However, in the hadronic models, the magnetic field strength is much larger, ranging from 10 G to 100 G [82]. For the convenience of study, we choose the parameter  $B_{T0} \simeq 1 \text{ G}$ . The different results can be inferred depending on the radiation models of blazars.

The current robust bound on  $g_{a\gamma}$  in the parameter region of interest here is provided by the CAST experiment, which constrains  $g_{a\gamma} < 6.6 \times 10^{-11} \text{ GeV}^{-1}$  for  $m_a < 0.02 \text{ eV}$  [83]. Other researches also set stronger constraint depending on specific procedures (e.g., [84–87]). In this work, we choose  $g_{a\gamma} = 5 \times 10^{-11} \text{ GeV}^{-1}$  allowed by the CAST bound as the benchmark value.

In the rest of this section, we discuss the validity of the weak-mixing condition. The first condition of Eq. (24) requires

$$\frac{B_T}{1\text{G}} \frac{1\text{cm}^{-3}}{n_e} \ll 1.45 \left( \frac{5 \times 10^{-11} \text{ GeV}^{-1}}{g_{a\gamma}} \right) \left( \frac{1\text{eV}}{E} \right). \quad (41)$$

In the case of blazar, this means that the weak-mixing condition is satisfied for

$$r \ll 28\text{kpc} \left( \frac{1\text{G}}{B_{T0}} \right) \left( \frac{n_{e0}}{5 \times 10^4 \text{ cm}^{-3}} \right) \left( \frac{r_E}{0.05 \text{ pc}} \right) \times \left( \frac{5 \times 10^{-11} \text{ GeV}^{-1}}{g_{a\gamma}} \right) \left( \frac{2 \text{ eV}}{E'} \right) \left( \frac{\delta}{15.64} \right). \quad (42)$$

where  $\delta$  is the relativistic Doppler factor and  $E'$  is the energy of photons in the rest frame. The observed energy  $E' \simeq 2$  eV corresponds to the photons in the optical waveband, and  $\delta = 15.64$  is taken to be the same typical value as [50]. Straightforwardly, the more stringent constraint on  $g_{a\gamma}$  is required for the larger magnetic field strength to meet the condition above.

The second condition of Eq. (24) constrains the mass of the ALP and the size of the jet,

$$m_a \ll 3.755 \times 10^{-11} \text{ eV} \left( \frac{n_e}{1 \text{ cm}^{-3}} \right)^{1/2}. \quad (43)$$

Thus, the ALPs considered here need to be very light as  $m_a \lesssim 10^{-13}$  eV, in order to satisfy the weak-mixing condition through the jet.

## B. Results

Given the field configuration of the BL Lacs and parameters of ALPs, we can neglect the second part of Eq. (36) and obtain

$$\begin{aligned} & V(r) - V(r_E) \\ &= -\frac{m_e g_{a\gamma}^2 \mathcal{V} E' B_{T0}^2}{8\pi\alpha \delta n_{e0}} (r - r_E) \\ &\simeq -0.134 \mathcal{V} \left( \frac{g_{a\gamma}}{5 \times 10^{-11} \text{ GeV}^{-1}} \right)^2 \left( \frac{E'}{2 \text{ eV}} \right) \left( \frac{15.64}{\delta} \right) \\ &\quad \times \left( \frac{B_{T0}}{1 \text{ G}} \right)^2 \left( \frac{5 \times 10^4 \text{ cm}^{-3}}{n_{e0}} \right) \left( \frac{r}{1 \text{ kpc}} \right). \end{aligned} \quad (44)$$

Though we choose the electron density to be the typical value in the above equations, it varies among different objects. In the SED model, a power-law distribution of relativistic electrons and/or pairs with low and upper energy cutoffs at  $\gamma_1$  and  $\gamma_2$ , respectively, and the power-law index  $q$  is presumed generally [82, 88]. In order to infer the electron density from the SED fitting, we assume a broken power-law distribution of electrons with index  $p$  for non-relativistic electrons [89],

$$n_e(\gamma) = \begin{cases} n_{e0} \gamma^{-p} & \text{for } 1 \leq \gamma < \gamma_1 \\ n_{e0} \gamma_1^{q-p} \gamma^{-q} & \text{for } \gamma_1 \leq \gamma \leq \gamma_2 \\ 0 & \text{else} \end{cases}, \quad (45)$$

where  $\gamma$  is the lorentz factor of the electrons. The index  $p$  is chosen to be the typical value of 2 hereafter [90]. In addition, assuming  $B_{T0} \approx B_0$  at the emission region, we can modify Eq. (44) with

$$\begin{aligned} & \left( \frac{B_{T0}}{1 \text{ G}} \right)^2 \left( \frac{5 \times 10^4 \text{ cm}^{-3}}{n_{e0}} \right) \approx \epsilon_{Be} f_\gamma, \\ & \epsilon_{Be} \equiv L_B / L_e, \\ & f_\gamma \equiv \frac{\gamma_2^{2-q} - \gamma_1^{2-q}}{(2-q) \gamma_1^{p-q}}, \end{aligned} \quad (46)$$

where  $\epsilon_{Be}$  is the ratio of the power carried in the magnetic field and the kinetic power in relativistic electrons, and  $f_\gamma$  accounts for the factor related to the electron density.

In the realistic calculation, we numerically solve Eq. (16) and show results in FIG. 1 for an illustration. Without loss of generality, we assume the initial photons linearly polarize along the  $y$ -axis, i.e.,  $\psi = 0$ , with a polarization degree  $\Pi_L = 0.3$ , and the polarization density matrix  $\rho_0 = \text{diag}(0.65, 0.35, 0)$ . The direction of the transverse magnetic field is chosen to be  $\phi = 3\pi/4$ , which maximizes the effect of ALPs and leads to  $\mathcal{V} = -\Pi_L = -0.3$ . We take  $m_a = 10^{-15}$  eV and set other relevant parameters as their typical values. In the numerical calculation, the length of domains along  $z$  are determined such that the magnetic field decreases by the decrease ratio  $\mathcal{R}$  from one domain to the next, i.e.,  $\mathcal{R} = 1 - B_{i+1}/B_i$  with the subscription denoting the  $i$ -th domain. In FIG. 1, we have set  $\mathcal{R} = 0.001$ .

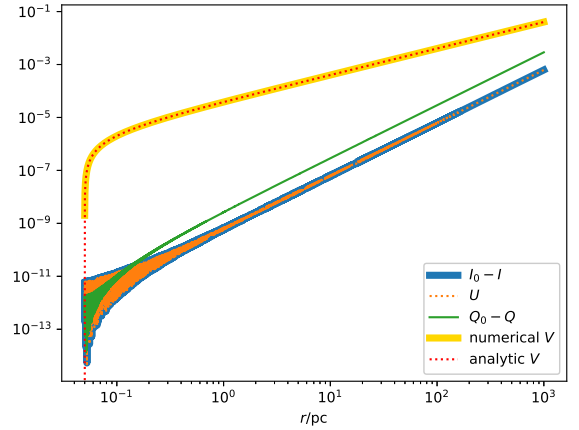


FIG. 1. Stokes parameters of photons along the jet with the subscription 0 refer to the initial values.

From FIG. 1, we can see that the analytic result of  $V$ , i.e., Eq. (44), is consistent with the numerical result. This justifies our analytic formulas. In order to have a deeper understanding for why ALPs can induce a much larger CP compared with LP, we make some qualitative analyses here. As long as  $P_{\gamma \rightarrow a}$  is small, the LP generated by dichroism can be approximated to be the conversion probability, i.e., Eq. (19) [47, 71]

$$\Delta \Pi_L = P_{\gamma \rightarrow a} \simeq \sin^2(2\theta) \sin^2(\xi/2), \quad (47)$$

where  $\xi = L/l_{\text{osc}}$  is the ratio of coherent length of magnetic field to oscillation length. The polarization-dependent phase shift (retardance) of photons induced by ALPs is

$$\phi_a \simeq \sin^2(2\theta)(\xi - \sin \xi). \quad (48)$$

If  $\phi_a \ll 1$ , then the phase shift results in the CP

$$V = Q_0 \sin \phi_a \simeq Q_0 \phi_a, \quad (49)$$



adopting the convention of  $U_0 = 0$  and  $Q_0 > 0$ . In the BL Lacs considered here, the oscillation length

$$l_{\text{osc}} = \Delta_{\text{osc}}^{-1} \approx |\Delta_{\text{pl}}|^{-1} \approx 9 \times 10^{-4} \text{pc} \left( \frac{E}{1 \text{eV}} \right) \left( \frac{1 \text{cm}^{-3}}{n_e} \right). \quad (50)$$

It is obvious that the oscillation length is far less than the scale of the jet  $l_{\text{osc}} \ll r_{\text{max}}$ , supposing the magnetic field is coherent over the entire jet region. Thus, the CP produced by mixing is much larger than that of LP. Eq. (47) also explains the oscillatory behavior of  $I$  and  $U$  in FIG. 1.

In FIG. 2 we calculate a similar case, in which all parameters retain unchanged except  $m_a = 10^{-11} \text{eV}$ . As shown in FIG. 2, when  $n_e$  approaches  $1 \text{cm}^{-3}$ , crossing the turning point where the resonant conversion occurs, the behavior of mixing is totally different since the weak-mixing condition Eq. (43) is no longer satisfied and hence Eq. (44) is not applicable.

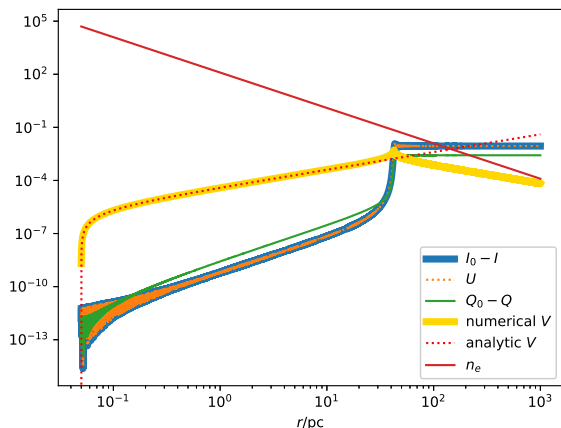


FIG. 2. Same as FIG. 1 except for  $m_a = 10^{-11} \text{eV}$

The optical CP in blazars is rarely detected [71, 91, 92]. Hutsemékers et al. [71] reported null detection of CP with typical uncertainties  $< 0.1\%$  in 21 quasars except for two highly polarized blazars. There has not been a confident detection of the optical CP in BL Lacs so far. Yet, some researches indicate a possible detection in 3C 66A [93, 94]. We will discuss these possible CP observation later. Provided CP constraints at the level of  $\sim 0.1\%$ , Eq. (44) directly gives a constraint  $g_{a\gamma} \cdot B_{T0} \lesssim 7.9 \times 10^{-12} \text{G} \cdot \text{GeV}^{-1}$ , i.e.,  $g_{a\gamma} \lesssim 7.9 \times 10^{-12} \text{GeV}^{-1}$  for  $B_{T0} = 1 \text{G}$ . In general, hadronic models require a higher magnetic field strength and less electron density than leptonic models, then the coupling between the ALP and photons is severely constrained. For example,  $B_{T0} \sim 10 \text{G}$  would require  $g_{a\gamma} \lesssim 7.9 \times 10^{-13} \text{GeV}^{-1}$  assuming the same electron density. In other words, if light ALPs are found, the radiation models with high magnetic field strength could be excluded. We also show the bounds

obtained in different situations in FIG. 3, in comparison with some previous bounds in the literature.

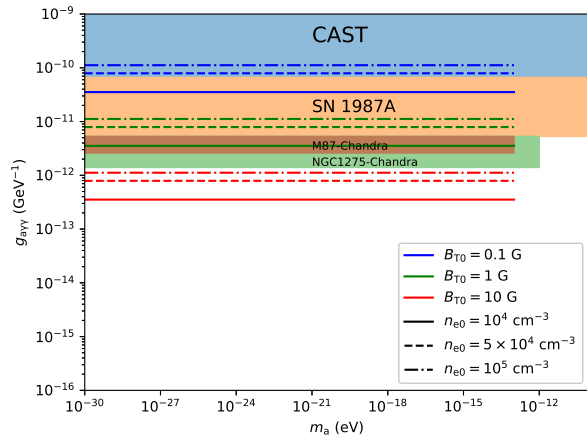


FIG. 3. Bounds on the ALP-photon coupling in comparison to previously obtained bounds [83, 85–87].

It is worth noting that the above constraints are estimated in the optimal case  $\mathcal{V} = \pm \Pi_L$ , which is supposed to be smaller in real. More detailed discussions on this are given in Sec. VB. The results obtained here are only rough estimation, and limited by the knowledge of the jet field configuration of BL Lacs and the precision of the optical CP measurement. There is no doubt that the further researches of BL Lacs and the improvement of future CP measurements in the optical band will significantly improve our results.

#### IV. ALP INTERPRETATION OF THE POSSIBLE CP OBSERVATION

There are few observations on the optical CP in blazars. Tommasi et al. [94] reported a marginal detection of the optical CP at  $2\sigma$  level in V and R bands for 3C 66A, using the Nordic Optical Telescope in 2001. An upper limit of  $0.4\%$  at  $3\sigma$  confidence level on CP was given. A  $3-6\sigma$  detection of CP with larger values in this BL Lacs was claimed by Takalo & Sillanpaa [93], using the same telescope in 1993. Besides, Hutsemékers et al. [71] reported small but significant optical CP effects in two blazars with uncertainties  $< 0.1\%$ . Given the above observations, we analyze the possible CP detection with the ALP assumption here. Since the two blazars in [71] are not BL Lacs, the model adopted in Sec. III A may not be applicable for them. We put these two objects aside and study the possibility that ALPs generate the detected CP in 3C 66A at first. We only analyze the data given by Takalo & Sillanpaa, considering that the state of LP was uncertain and the amount of data is inadequate in the research of Tommasi et al.

The handedness of CP changed during the measurement in [93]. This implies that  $\phi - \psi \approx k\pi/2$  with  $k \in \mathbb{Z}$  in the ALP scenario. Hence, we can make the approximation  $\mathcal{V} \approx 2\Pi_L(\phi - \psi)$  in Eq. (36) and obtain

$$\frac{\Pi_C}{\Pi_L E'} \propto g_{a\gamma}^2 \epsilon_{Be} f_\gamma \delta^{-1} r_{\max}(\psi - \phi). \quad (51)$$

The observations were made in the UBVRI photometric systems. Taking into account the effective energy of the color bands, we implement a linear polynomial fit between  $\Pi_C/(\Pi_L E')$  and the polarization angle  $\psi$ . The results are shown in FIG. 4 and TABLE. I. Here, we have supposed that the orientation of the magnetic field is fixed. Owing to the small value of CP, the quality of our analysis is sensitive to the accuracy of the polarization angle. It can be seen from FIG. 4 that the data points of RI bands are distributed differently from those of UBV bands. This may be attributed to the systematic differences caused by the two kinds of photomultiplier tubes in the UBV and RI channels. Physical processes that result in the energy dependent rotation of the polarization angle can also affect the distribution. We consider two cases here: one includes the RI bands, while the other not. The potential rotation of the photon polarization angle generated by other effects in the propagation through the astronomical space is neglected in the fitting.

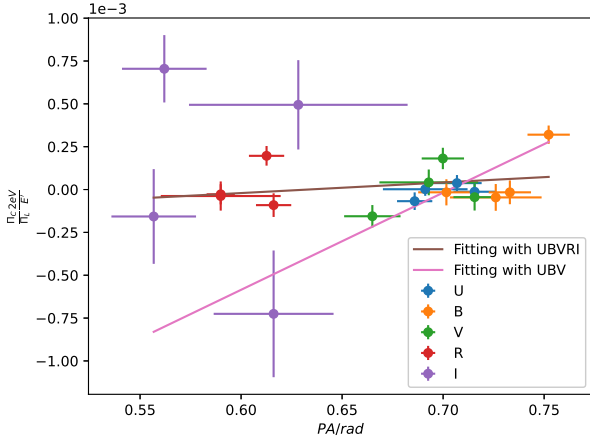


FIG. 4. Linear polynomial fit to observation in 3C 66A in [93]. The letters UBVRI represent different band filters.

Bands	$a_0$	$\sigma_{a_0}$	$a_1$	$\sigma_{a_1}$
UBVRI	-0.39	0.45	0.62	0.66
UBV	-4.0	1.1	5.7	1.6

TABLE I. Coefficients of linear polynomial fit to observation in 3C 66A in form of  $y = a_0 + a_1 x$ . Parameters are in unit of  $10^{-3}$

As shown in TABLE. I, no clear physical conclusion can be drawn from the fit in the UBVRI case, due to

the large standard error compared to the corresponding fitting parameters. In the UBV case, the direction of the transverse magnetic field of the jet  $\phi$  is estimated to be 0.70 rad (40.3°) or 3.84 rad (220.4°). From the slope of the line, we obtain

$$g_{a\gamma} \approx 7 \times 10^{-12} \text{ GeV}^{-1} \left[ \epsilon_{Be} f_\gamma \left( \frac{15.64}{\delta} \right) \left( \frac{r_{\max}}{1 \text{ kpc}} \right) \right]^{-1/2}. \quad (52)$$

The jet model fitting to the observed SED and optical variability patterns of 3C 66A usually gives  $\delta \sim 30$  and  $f_\gamma \approx 1$  [82, 95, 96]. In the leptonic models, a pure SSC model would require a tiny equipartition ratio  $\epsilon_{Be} \sim 10^{-3}$ , while in the EC+SSC models  $\epsilon_{Be}$  would be rather larger  $\sim 0.1$  [82, 95]. Consequently, the EC+SSC models give  $g_{a\gamma} \approx 3 \times 10^{-11} \text{ GeV}^{-1} \sqrt{1 \text{ kpc}/r_{\max}}$ , which is close to the CAST bound, while the ALP interpretation in the pure SSC model is excluded by CAST. In the hadronic models with the equipartition ratio  $\epsilon_{Be} \sim 25$  [82], we can get  $g_{a\gamma} \approx 2 \times 10^{-12} \text{ GeV}^{-1} \sqrt{1 \text{ kpc}/r_{\max}}$ .

Apart from 3C 66A, Takalo & Sillanpaa indicated a rapid variability in the U-band CP during the observation of OJ 287. Although the nightly average CP observation did not find the optical CP, we can still repeat the above analysis procedure for this object, and provide the results in FIG. 5 and TABLE. II. Similarly, we get a model-dependent estimation for  $g_{a\gamma}$ , listing in TABLE. III.

The observations of these objects indicate a similar estimation for  $g_{a\gamma}$ , which is about a few orders of  $10^{-12} \text{ GeV}^{-1}$ . However, we emphasize that the validity of such results strongly depends on the accuracy of the optical polarimetry. Simultaneous LP and CP measurements in the optical band with high accuracy are needed to verify this analysis in the future.

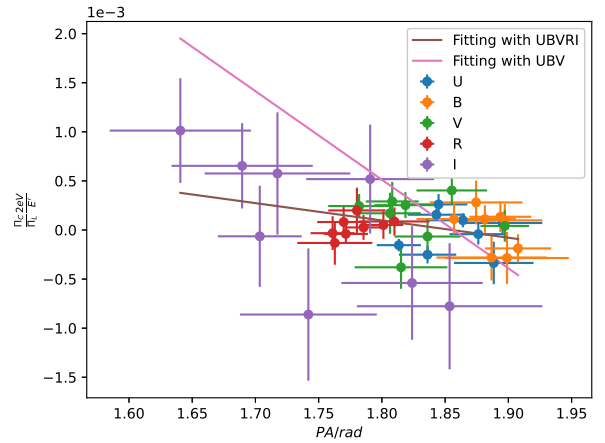


FIG. 5. Linear polynomial fit to observation in OJ 287 in [93]. The letters UBVRI represent different band filters.

Bands	$a_0$	$\sigma_{a_0}$	$a_1$	$\sigma_{a_1}$
UBVRI	3.3	1.5	-1.8	0.79
UBV	16.8	6.4	-9.0	3.5

TABLE II. Coefficients of linear polynomial fit to observation in OJ 287 in form of  $y = a_0 + a_1x$ . Parameters are in unit of  $10^{-3}$

Bands	$\phi(rad)$	$g_{a\gamma}(10^{-12} \text{ GeV}^{-1})$	Leptonic	Hadronic
UBVRI	0.26 or 3.40	1.3	0.70	
UBV	0.30 or 3.44	2.9	1.6	

TABLE III. Estimation of  $g_{a\gamma}$  using fitting coefficients in OJ 287. The factor  $\sqrt{1 \text{ kpc}/r_{\text{max}}}$  in  $g_{a\gamma}$  is omitted.  $\delta = 15$ .  $f_\gamma \approx 1.2$ ,  $\epsilon_{Be} = 8.2$  for leptonic model and  $f_\gamma \approx 0.5$ ,  $\epsilon_{Be} = 66$  for hadronic model [82].

## V. DISCUSSIONS

As mentioned in the former section, Eq. (44) is idealized in some sense. In this section, we discuss some relevant physical factors that affect the above results.

### A. Intrinsic CP

On the astrophysical origin of optical CP in blazars, the inverse Compton scattering of radio photons with high CP and the intrinsic CP are two likely options [62]. However, the former mechanism requires the significant radio CP and SSC contribution to optical continuum, which are not observed. Therefore, we discuss the consequence that the intrinsic CP is present in this subsection.

The synchrotron radiation of particles generates a small degree of intrinsic CP with  $\Pi_C \propto \nu^{-1/2}$  [97, 98]. In a pure electron-positron plasma, the CP component cancels, leaving only the LP component. Assuming an electron-positron-proton plasma with  $f$  denoting the fraction of the positron in the jet, the degree of the intrinsic CP can be characterized as [62]

$$\Pi_C \approx 2.8 \times 10^{-2} \left( \frac{B}{1 \text{ G}} \right)^{\frac{1}{2}} \left( \frac{1 \text{ eV}}{E'} \right)^{\frac{1}{2}} \left( \frac{\Pi_L}{0.71} \right) \left( \frac{\Gamma}{15} \right)^{\frac{3}{2}} (1-2f), \quad (53)$$

where the Lorentz factor  $\Gamma$  can be approximated by  $\delta$  in the highly collimated regime. Detecting upper limits of the intrinsic CP of two blazars, Liodakis et al. [99] claimed the exclusion of high-energy emission models with the high magnetic field strength and low positron fraction, like the hadronic models.

However, the ALP induced CP may offset the intrinsic CP since the handness of ALP induced CP can be positive or negative, which is determined by the angle between the magnetic field and photon polarization. From the view of the observer, the handness of CP is positive, if the direction of the transverse magnetic field lies

in *I, III* quadrants of the Cartesian coordinate system with the direction of polarization as the x-axis. Thus, we study the case that ALPs induce a negative CP in the hadronic model. We calculate the sum of two kinds of CP origins with  $B$  in the range of  $[0, 10]$  G and  $[0, 0.5)$  for  $f$ . In order to get comparable values, we choose  $g_{a\gamma} = 5 \times 10^{-12} \text{ GeV}^{-1}$  and  $\phi = \pi/4$  while keeping other parameters unchanged. As shown in FIG. 6, there exists a large parameter region where the optical CP does not exceed the precision of measurements even for the large magnetic field strength and low positron fraction. Smaller coupling  $g_{a\gamma}$  indicates the possibility of larger magnetic field. In order to discriminate these two scenarios, it is crucial to measure the radio and optical CP simultaneously. This is because that the radio CP is expected to be associated with the intrinsic CP, while ALPs considered here have little effect on the radio photons.

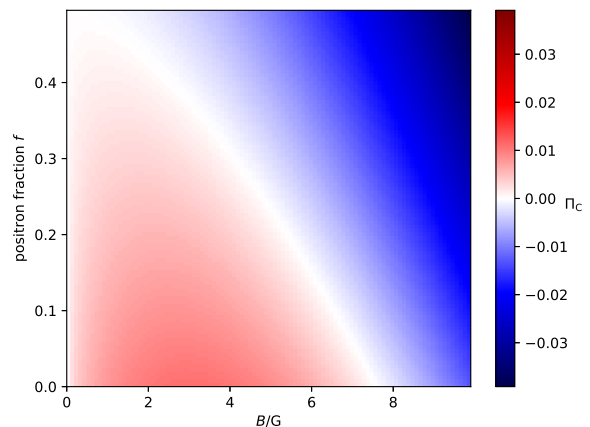


FIG. 6. Optical CP with different magnetic field strength and plasma composition. The colorbar represents degree of CP. Details of parameters are stated in the text.

### B. Structure of the jet

In the above analysis, the angle of the magnetic field is idealized, fixing to  $3\pi/4$  or  $\pi/4$ . A realistic CP must be smaller than these cases. Besides, the angle could vary in the propagation, resulting in a shorter coherent length. In order to estimate the effect of the varied angle, we assume that the direction of magnetic field is partially random in each calculation domain

$$\phi = \phi_0 + \alpha \Delta\phi, \quad (54)$$

where  $\phi_0 = 3\pi/4$  and  $\Delta\phi$  is a uniform random variable in the range of  $[-\pi, \pi]$ . The factor  $\alpha$  characterizes the degree of randomness. Similar to what we have done in III B, the evolution of the Stokes parameters with  $\alpha = 0.1, 0.2, 0.3$  and  $\mathcal{R} = 0.001, 0.01, 0.1$  are calculated.



FIG. 7 presents the results in these cases. The coherent length of the magnetic field (also the number of domains) is determined by the decrease ratio  $\mathcal{R}$ . As shown in FIG. 7, the values of  $\alpha$  and  $\mathcal{R}$  significantly change the pattern of the evolution. As  $\alpha$  increases, smaller the coherent length is, the more important role it plays, and more randomness and quiver shows. Moreover, we draw the distribution of CP of 1000 different magnetic field realization for each parameter case in FIG. 8. It can be seen from FIG. 8 that in a more realistic field configuration, the values of CP are smaller than the optimal case, but the magnitude of CP hardly changes.

In order to comprehend the results in FIG. 7 and FIG. 8, we suppose  $\alpha \ll 1$  and rephrase Eq. (38)

$$\mathcal{V}_{n+1} \approx \Pi_L \sin 2(\phi_0 - \psi_n) + 2\alpha \Delta\phi_n \Pi_L \cos 2(\phi_0 - \psi_n), \quad (55)$$

where the subscription  $n$  indicates the serial number of the domain. Then the change of  $V$  is determined by two parts: the incremental part (the former term of the RHS) and the random part (the latter term of the RHS). Also, Eq. (36) is applicable for the incremental part in each domain, which explains the magnitude of the expectation value of the CP distribution in our choice of  $\phi_0$ . In the  $\phi_0 = 3\pi/4$  case, the second term can be written as  $-2\alpha \Delta\phi_n U_n$ . Hence, as shown in FIG. 7, the quiver of  $V$  in the propagation is related to  $U$  with a domain delay. The contribution of the random part can be treated as a random walk, thus the variance of the distribution is estimated to be  $2\alpha \langle \Delta\phi_n U_n \rangle \sqrt{N}$ , where  $N$  is the number of domains and the angle bracket means the expectation value.

In addition, the propagation space of beams may be not line-shaped, but be like a column covering a certain region of magnetic field with different direction. If the direction angle of the magnetic field evenly varies from  $\phi_1$  to  $\phi_2$  in the region, the magnitude of CP can be estimated by replacing  $\mathcal{V}$  in Eq. (36) with  $\int_{\phi_1}^{\phi_2} \mathcal{V}(\phi) d\phi / (\phi_2 - \phi_1)$ , assuming the initial photons from different positions have the same polarization state. FIG. 9 shows the distribution of assembly CP for beams propagating in a partially random magnetic field region, where  $\phi_0$  evenly varies in an interval. The decrease ratio is chosen to be  $\mathcal{R} = 0.1$  for simplicity. The assembly CP significantly cancels in the first two subfigures, while the third case shows a moderate CP. This means that the appearance of ALP induced CP has a requirement on the structure of the jet or the high resolution of the measurement.

### C. CP in other astrophysical magnetic fields

Magnetic fields are ubiquitous in the propagation of photons from blazars to earth. The ALP-photon mixing in other astrophysical magnetic fields could contribute to the optical CP, altering the results obtained above. Without any doubt, we should have a basic awareness of the effects. In order to make a simple estimation, the

contribution of mixing is  $\sim \Pi_L g_{a\gamma}^2 B^2 l_{\text{osc}} L$  from Eq. (49) as long as the weak-mixing condition is fulfilled. So we can define a factor as

$$f_{\text{CP}} = \left( \frac{B}{1 \text{ G}} \right)^2 \left( \frac{5 \times 10^4 \text{ cm}^{-3}}{n_e} \right) \left( \frac{L}{1 \text{ kpc}} \right), \quad (56)$$

which straightforwardly characterizes the CP contribution of the ALP-photon mixing compared to that in the jets of blazars. Owing to the structure of the jet model, the distance dependence of the magnetic field and of the electron density cancel each other, leaving  $f_{\text{CP}} = 1$  in BL Lacs. We evaluate the factor  $f_{\text{CP}}$  in the magnetic field inside a galaxy cluster (intra-cluster magnetic field, ICMF), the intergalactic magnetic field (IGMF), and the galactic magnetic field in the Milky Way (GMF), presenting in TABLE. IV with typical values. It should be noted that a turbulent configuration of the field is usually used in these fields. Then, the situation is more close to the random walk case that we discuss in the former part, and the output relies on the specific realization of the magnetic field. As we can see in TABLE. IV, the contribution of the mixing can be neglected in other astrophysical magnetic fields.

Scenarios	$B(\text{G})$	$n_e(\text{cm}^{-3})$	$L(\text{kpc})$	$f_{\text{CP}}$
ICMF [100, 101]	$10^{-6}$	$10^{-3}$	10	$5 \times 10^{-4}$
IGMF [102–105]	$10^{-9}$	$10^{-7}$	$5 \times 10^4$	$2.5 \times 10^{-2}$
GMF [106, 107]	$10^{-6}$	$10^{-1}$	$10^{-2}$	$5 \times 10^{-9}$

TABLE IV.  $f_{\text{CP}}$  in different magnetic field scenarios.

Apart from the astrophysical magnetic fields mentioned above, the field in the supercluster has been discussed in [48, 49]. The ALP-photon mixing in the supercluster was originally proposed to explain the alignments of the optical polarization of light from quasars in extremely large regions of the sky, but disfavored by subsequent study. The effect of the supercluster needs to be taken into account when it lies in the sight of blazars. The authors of [49] claimed to constrain  $g_{a\gamma} \lesssim 10^{-13} \text{ GeV}^{-1}$  for  $m_a \lesssim 10^{-14} \text{ eV}$ , which would be the most stringent limit to date. They assumed the electron density of  $\mathcal{O}(10^{-6}) \text{ cm}^{-3}$  and the magnetic field of  $\mathcal{O}(\mu\text{G})$  with the coherent length  $\sim 100 \text{ kpc}$  in the supercluster. This configuration of the supercluster field would give  $f_{\text{CP}} \sim 5$ . However, researches of the supercluster magnetic fields [108–113] find that they are filamentous. There is no firm conclusion about the magnetic field strength in galaxy filaments within the supercluster, neither from observations nor from theory [114–117]. It seems likely that the field strength in [49] was overestimated, and the strict constraint would be relaxed to some extent. Despite this, it will help restrict our results even if the optical CP is produced in the supercluster.

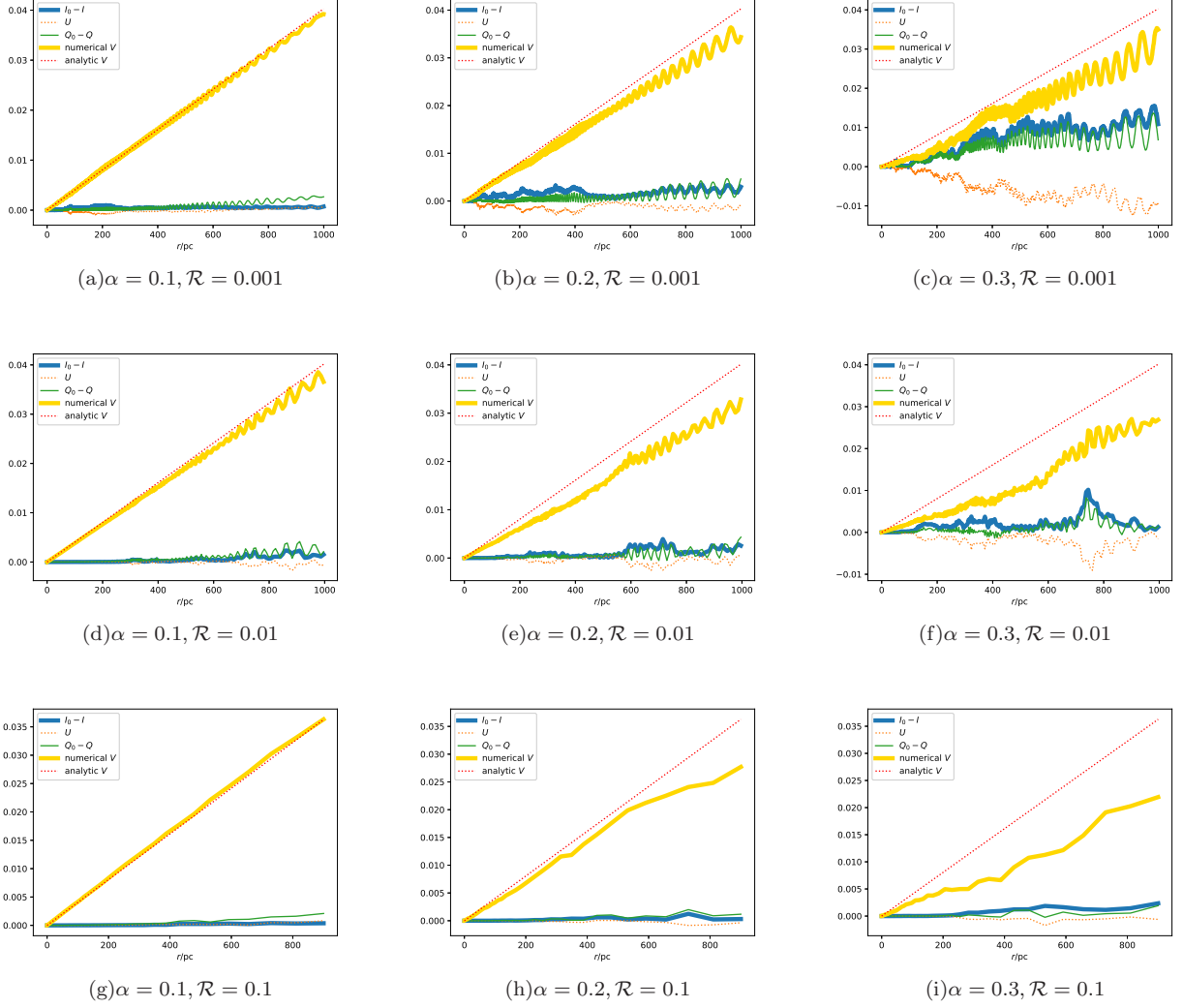


FIG. 7. Evolution of Stokes parameters for magnetic field with varied angle.

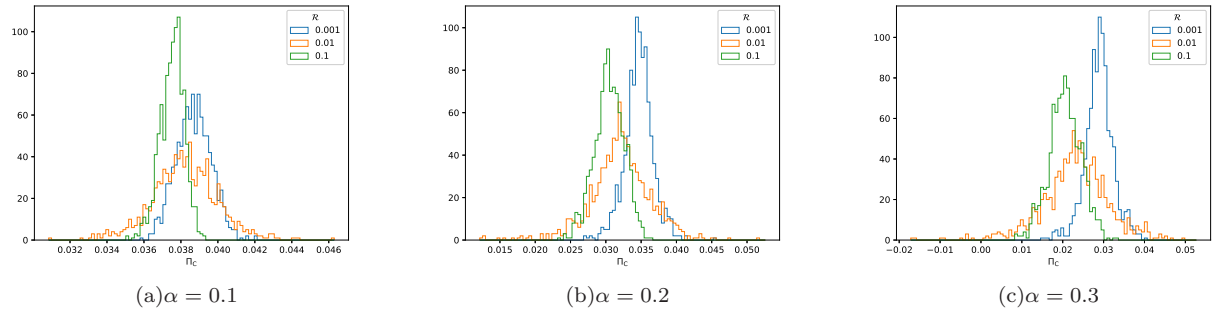


FIG. 8. Distribution of CP for magnetic field with varied angle.

## VI. CONCLUSIONS

In this work, we investigate a potential optical CP in blazars induced by the ALP-photon mixing. Although

this mixing is weak and has little effect on the flux and the LP of photons, we have shown that it could induce a considerable optical CP when the oscillation length is much less than the coherent length of the magnetic field in the blazar jet. The formulae of the ALP induced CP

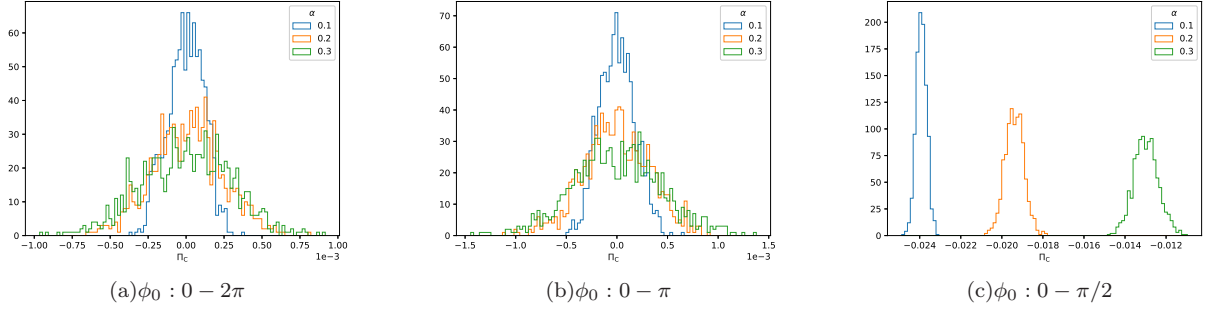


FIG. 9. Distribution of assembly CP.

in a simple conical jet are derived, which lead to a constraint on  $g_{a\gamma}$ , i.e.,  $g_{a\gamma} \cdot B_{T0} \lesssim 7.9 \times 10^{-12} \text{ G} \cdot \text{GeV}^{-1}$  for  $m_a \lesssim 10^{-13} \text{ eV}$ , corresponding to the upper limit on the observed CP at the level of  $\sim 0.1\%$ . Hence, the coupling between the ALP and photon would be significantly constrained in the hadronic radiation model with a large magnetic field strength in the jet. Further research on the BL Lacs and CP measurement in the optical band would significantly improve these results.

In particular, the possible CP observations of two blazar 3C 66A and OJ 287 induced by the ALP are analyzed using the data in the paper of Takalo & Sillanpaa. We find that these observations indicate a similar estimation of  $g_{a\gamma} \sim 10^{-12} \text{ GeV}^{-1}$ . Large amount of the simultaneous LP and CP measurements with high accuracy in the future is needed to verify the irregular results.

Though hadronic models set stringent constraint on  $g_{a\gamma}$ , the results could be significantly changed considering the intrinsic CP. Measuring the radio and optical CP simultaneously would be helpful to clarify the situation.

Besides, note that many results of the ALP induced CP in this work are derived with an idealized jet configuration. As stated in the last part of Sec.V, we have shown that the obtained results are partially valid in more realistic cases.

## ACKNOWLEDGMENTS

The authors would like to thank Zhao-Huan Yu, Zhuo Li, Kai Wang, Pu Du, and Jin Zhang for helpful discussions. The work is supported by the National Natural Science Foundation of China under grant No. 12175248. The work of JWW is supported by Natural Science Foundation of China under grant No. 12150610465 and the research grant "the Dark Universe: A Synergic Multi-messenger Approach" number 2017X7X85K under the program PRIN 2017 funded by the Ministero dell'Istruzione, Università e della Ricerca (MIUR).

- 
- [1] E. Witten, "Some Properties of O(32) Superstrings," *Phys. Lett. B* **149** (1984) 351–356.
  - [2] P. Svrcek and E. Witten, "Axions In String Theory," *JHEP* **06** (2006) 051, [arXiv:hep-th/0605206](#).
  - [3] J. P. Conlon, "The QCD axion and moduli stabilisation," *JHEP* **05** (2006) 078, [arXiv:hep-th/0602233](#).
  - [4] J. P. Conlon, "Seeing the Invisible Axion in the Sparticle Spectrum," *Phys. Rev. Lett.* **97** (2006) 261802, [arXiv:hep-ph/0607138](#).
  - [5] A. Arvanitaki, S. Dimopoulos, S. Dubovsky, N. Kaloper, and J. March-Russell, "String Axiverse," *Phys. Rev. D* **81** (2010) 123530, [arXiv:0905.4720 \[hep-th\]](#).
  - [6] B. S. Acharya, K. Bobkov, and P. Kumar, "An M Theory Solution to the Strong CP Problem and Constraints on the Axiverse," *JHEP* **11** (2010) 105, [arXiv:1004.5138 \[hep-th\]](#).
  - [7] M. Cicoli, M. Goodsell, and A. Ringwald, "The type IIB string axiverse and its low-energy phenomenology," *JHEP* **10** (2012) 146, [arXiv:1206.0819 \[hep-th\]](#).
  - [8] R. D. Peccei and H. R. Quinn, "CP Conservation in the Presence of Instantons," *Phys. Rev. Lett.* **38** (1977) 1440–1443.
  - [9] R. D. Peccei and H. R. Quinn, "Constraints Imposed by CP Conservation in the Presence of Instantons," *Phys. Rev. D* **16** (1977) 1791–1797.
  - [10] S. Weinberg, "A New Light Boson?," *Phys. Rev. Lett.* **40** (1978) 223–226.
  - [11] F. Wilczek, "Problem of Strong  $P$  and  $T$  Invariance in the Presence of Instantons," *Phys. Rev. Lett.* **40** (1978) 279–282.
  - [12] H.-Y. Cheng, "The Strong CP Problem Revisited," *Phys. Rept.* **158** (1988) 1.
  - [13] E. W. Kolb and M. S. Turner, *The Early Universe*, vol. 69. CRC Press, 1990.
  - [14] M. S. Turner, "Windows on the Axion," *Phys. Rept.* **197** (1990) 67–97.
  - [15] P. Sikivie, "Axion Cosmology," *Lect. Notes Phys.* **741** (2008) 19–50, [arXiv:astro-ph/0610440](#).

- [16] S. M. Carroll, “Quintessence and the rest of the world,” *Phys. Rev. Lett.* **81** (1998) 3067–3070, [arXiv:astro-ph/9806099](#).
- [17] D. J. E. Marsh, “Axion Cosmology,” *Phys. Rept.* **643** (2016) 1–79, [arXiv:1510.07633 \[astro-ph.CO\]](#).
- [18] P. W. Graham, I. G. Irastorza, S. K. Lamoreaux, A. Lindner, and K. A. van Bibber, “Experimental Searches for the Axion and Axion-Like Particles,” *Ann. Rev. Nucl. Part. Sci.* **65** (2015) 485–514, [arXiv:1602.00039 \[hep-ex\]](#).
- [19] M. A. Fedderke, P. W. Graham, and S. Rajendran, “Axion Dark Matter Detection with CMB Polarization,” *Phys. Rev. D* **100** (2019) 015040, [arXiv:1903.02666 \[astro-ph.CO\]](#).
- [20] D. J. Schwarz, J. Goswami, and A. Basu, “Geometric optics in the presence of axionlike particles in curved spacetime,” *Phys. Rev. D* **103** (2021) L081306, [arXiv:2003.10205 \[hep-ph\]](#).
- [21] W. DeRocco and A. Hook, “Axion interferometry,” *Phys. Rev. D* **98** (2018) 035021, [arXiv:1802.07273 \[hep-ph\]](#).
- [22] I. Obata, T. Fujita, and Y. Michimura, “Optical Ring Cavity Search for Axion Dark Matter,” *Phys. Rev. Lett.* **121** (2018) 161301, [arXiv:1805.11753 \[astro-ph.CO\]](#).
- [23] Y. Chen, J. Shu, X. Xue, Q. Yuan, and Y. Zhao, “Probing Axions with Event Horizon Telescope Polarimetric Measurements,” *Phys. Rev. Lett.* **124** (2020) 061102, [arXiv:1905.02213 \[hep-ph\]](#).
- [24] G.-W. Yuan, Z.-Q. Xia, C. Tang, Y. Zhao, Y.-F. Cai, Y. Chen, J. Shu, and Q. Yuan, “Testing the ALP-photon coupling with polarization measurements of Sagittarius A\*,” *JCAP* **03** (2021) 018, [arXiv:2008.13662 \[astro-ph.HE\]](#).
- [25] P. Sikivie, “Experimental Tests of the Invisible Axion,” *Phys. Rev. Lett.* **51** (1983) 1415–1417. [Erratum: *Phys.Rev.Lett.* 52, 695 (1984)].
- [26] G. Raffelt and L. Stodolsky, “Mixing of the Photon with Low Mass Particles,” *Phys. Rev. D* **37** (1988) 1237.
- [27] L. Maiani, R. Petronzio, and E. Zavattini, “Effects of Nearly Massless, Spin Zero Particles on Light Propagation in a Magnetic Field,” *Phys. Lett. B* **175** (1986) 359–363.
- [28] C. Csaki, N. Kaloper, M. Peloso, and J. Terning, “Super GZK photons from photon axion mixing,” *JCAP* **05** (2003) 005, [arXiv:hep-ph/0302030](#).
- [29] A. De Angelis, M. Roncadelli, and O. Mansutti, “Evidence for a new light spin-zero boson from cosmological gamma-ray propagation?,” *Phys. Rev. D* **76** (2007) 121301, [arXiv:0707.4312 \[astro-ph\]](#).
- [30] D. Hooper and P. D. Serpico, “Detecting Axion-Like Particles With Gamma Ray Telescopes,” *Phys. Rev. Lett.* **99** (2007) 231102, [arXiv:0706.3203 \[hep-ph\]](#).
- [31] M. Simet, D. Hooper, and P. D. Serpico, “The Milky Way as a Kiloparsec-Scale Axionscope,” *Phys. Rev. D* **77** (2008) 063001, [arXiv:0712.2825 \[astro-ph\]](#).
- [32] M. A. Sanchez-Conde, D. Paneque, E. Bloom, F. Prada, and A. Dominguez, “Hints of the existence of Axion-Like-Particles from the gamma-ray spectra of cosmological sources,” *Phys. Rev. D* **79** (2009) 123511, [arXiv:0905.3270 \[astro-ph.CO\]](#).
- [33] A. Mirizzi and D. Montanino, “Stochastic conversions of TeV photons into axion-like particles in extragalactic magnetic fields,” *JCAP* **12** (2009) 004, [arXiv:0911.0015 \[astro-ph.HE\]](#).
- [34] N. Bassan, A. Mirizzi, and M. Roncadelli, “Axion-like particle effects on the polarization of cosmic high-energy gamma sources,” *JCAP* **05** (2010) 010, [arXiv:1001.5267 \[astro-ph.HE\]](#).
- [35] A. De Angelis, G. Galanti, and M. Roncadelli, “Relevance of axion-like particles for very-high-energy astrophysics,” *Phys. Rev. D* **84** (2011) 105030, [arXiv:1106.1132 \[astro-ph.HE\]](#). [Erratum: *Phys.Rev.D* 87, 109903 (2013)].
- [36] G. Galanti, F. Tavecchio, M. Roncadelli, and C. Evoli, “Blazar VHE spectral alterations induced by photon-ALP oscillations,” *Mon. Not. Roy. Astron. Soc.* **487** (2019) 123–132, [arXiv:1811.03548 \[astro-ph.HE\]](#).
- [37] M. S. Pshirkov and S. B. Popov, “Conversion of Dark matter axions to photons in magnetospheres of neutron stars,” *J. Exp. Theor. Phys.* **108** (2009) 384–388, [arXiv:0711.1264 \[astro-ph\]](#).
- [38] A. Hook, Y. Kahn, B. R. Safdi, and Z. Sun, “Radio Signals from Axion Dark Matter Conversion in Neutron Star Magnetospheres,” *Phys. Rev. Lett.* **121** (2018) 241102, [arXiv:1804.03145 \[hep-ph\]](#).
- [39] F. P. Huang, K. Kadota, T. Sekiguchi, and H. Tashiro, “Radio telescope search for the resonant conversion of cold dark matter axions from the magnetized astrophysical sources,” *Phys. Rev. D* **97** (2018) 123001, [arXiv:1803.08230 \[hep-ph\]](#).
- [40] C. Dessert, A. J. Long, and B. R. Safdi, “X-ray Signatures of Axion Conversion in Magnetic White Dwarf Stars,” *Phys. Rev. Lett.* **123** (2019) 061104, [arXiv:1903.05088 \[hep-ph\]](#).
- [41] J. Darling, “Search for Axionic Dark Matter Using the Magnetar PSR J1745-2900,” *Phys. Rev. Lett.* **125** (2020) 121103, [arXiv:2008.01877 \[astro-ph.CO\]](#).
- [42] T. D. P. Edwards, B. J. Kavanagh, L. Visinelli, and C. Weniger, “Transient Radio Signatures from Neutron Star Encounters with QCD Axion Miniclusters,” *Phys. Rev. Lett.* **127** (2021) 131103, [arXiv:2011.05378 \[hep-ph\]](#).
- [43] J.-W. Wang, X.-J. Bi, R.-M. Yao, and P.-F. Yin, “Exploring axion dark matter through radio signals from magnetic white dwarf stars,” *Phys. Rev. D* **103** (2021) 115021, [arXiv:2101.02585 \[hep-ph\]](#).
- [44] J.-W. Wang, X.-J. Bi, and P.-F. Yin, “Detecting axion dark matter through the radio signal from Omega Centauri,” *Phys. Rev. D* **104** (2021) 103015, [arXiv:2109.00877 \[astro-ph.HE\]](#).
- [45] A. Prabhu, “Axion production in pulsar magnetosphere gaps,” *Phys. Rev. D* **104** (2021) 055038, [arXiv:2104.14569 \[hep-ph\]](#).
- [46] C. Dessert, D. Dunsky, and B. R. Safdi, “Upper limit on the axion-photon coupling from magnetic white



- dwarf polarization,” *Phys. Rev. D* **105** (2022) 103034, [arXiv:2203.04319 \[hep-ph\]](#).
- [47] P. Jain, S. Panda, and S. Sarala, “Electromagnetic polarization effects due to axion photon mixing,” *Phys. Rev. D* **66** (2002) 085007, [arXiv:hep-ph/0206046](#).
- [48] A. Payez, J. R. Cudell, and D. Hutsemekers, “Can axion-like particles explain the alignments of the polarisations of light from quasars?,” *Phys. Rev. D* **84** (2011) 085029, [arXiv:1107.2013 \[astro-ph.CO\]](#).
- [49] A. Payez, J. R. Cudell, and D. Hutsemekers, “New polarimetric constraints on axion-like particles,” *JCAP* **07** (2012) 041, [arXiv:1204.6187 \[astro-ph.CO\]](#).
- [50] M. Meyer, D. Montanino, and J. Conrad, “On detecting oscillations of gamma rays into axion-like particles in turbulent and coherent magnetic fields,” *JCAP* **09** (2014) 003, [arXiv:1406.5972 \[astro-ph.HE\]](#).
- [51] F. Tavecchio, M. Roncadelli, and G. Galanti, “Photons to axion-like particles conversion in Active Galactic Nuclei,” *Phys. Lett. B* **744** (2015) 375–379, [arXiv:1406.2303 \[astro-ph.HE\]](#).
- [52] F. Day and S. Krippendorff, “Searching for Axion-Like Particles with X-ray Polarimeters,” *Galaxies* **6** (2018) 45, [arXiv:1801.10557 \[hep-ph\]](#).
- [53] G. Galanti, “Photon-ALP interaction as a measure of initial photon polarization,” *Phys. Rev. D* **105** (2022) 083022, [arXiv:2202.10315 \[hep-ph\]](#).
- [54] G. Galanti, “Photon-ALP oscillations inducing modification on  $\gamma$ -ray polarization,” [arXiv:2202.11675 \[astro-ph.HE\]](#).
- [55] G. Galanti, M. Roncadelli, and F. Tavecchio, “ALP induced polarization effects on photons from galaxy clusters,” [arXiv:2202.12286 \[astro-ph.HE\]](#).
- [56] S. Shakeri and F. Hajkarim, “Probing Axions via Light Circular Polarization and Event Horizon Telescope,” [arXiv:2209.13572 \[hep-ph\]](#).
- [57] H. S. Krawczynski *et al.*, “X-Ray Polarimetry with the Polarization Spectroscopic Telescope Array (PolSTAR),” *Astropart. Phys.* **75** (2016) 8, [arXiv:1510.08358 \[astro-ph.IM\]](#).
- [58] P. Soffitta, “IXPE the Imaging X-ray Polarimetry Explorer,” in *UV, X-Ray, and Gamma-Ray Space Instrumentation for Astronomy XX*, O. H. Siegmund, ed., vol. 10397, p. 103970I, International Society for Optics and Photonics. SPIE, 2017, <https://doi.org/10.1117/12.2275485>.
- [59] C. M. Urry and P. Padovani, “Unified schemes for radio-loud active galactic nuclei,” *Publ. Astron. Soc. Pac.* **107** (1995) 803, [arXiv:astro-ph/9506063](#).
- [60] J. R. P. Angel and H. S. Stockman, “Optical and infrared polarization of active extragalactic objects,” *Ann. Rev. Astron. Astrophys.* **18** (1980) 321–361.
- [61] H. Zhang, “Blazar Optical Polarimetry: Current Progress in Observations and Theories,” *Galaxies* **7** (2019) 85.
- [62] F. M. Rieger and K. Mannheim, “On the Possible Origin of Optical Circular Polarization in Blazars,” *Chinese Journal of Astronomy and Astrophysics* **5** (Dec, 2005) 317–319, [arXiv:1701.00271 \[astro-ph.HE\]](#).
- [63] M. Kuster, G. Raffelt, and B. Beltran, eds., *Axions: Theory, cosmology, and experimental searches. Proceedings, 1st Joint ILIAS-CERN-CAST axion training, Geneva, Switzerland, November 30-December 2, 2005*, vol. 741. 2008.
- [64] G. Galanti and M. Roncadelli, “Behavior of axionlike particles in smoothed out domainlike magnetic fields,” *Phys. Rev. D* **98** (2018) 043018, [arXiv:1804.09443 \[astro-ph.HE\]](#).
- [65] J. Davies, M. Meyer, and G. Cotter, “Relevance of jet magnetic field structure for blazar axionlike particle searches,” *Phys. Rev. D* **103** (2021) 023008, [arXiv:2011.08123 \[astro-ph.HE\]](#).
- [66] A. Dobrynina, A. Kartavtsev, and G. Raffelt, “Photon-photon dispersion of TeV gamma rays and its role for photon-ALP conversion,” *Phys. Rev. D* **91** (2015) 083003, [arXiv:1412.4777 \[astro-ph.HE\]](#). [Erratum: *Phys.Rev.D* **95**, 109905 (2017)].
- [67] A. Kosowsky, “Cosmic microwave background polarization,” *Annals Phys.* **246** (1996) 49–85, [arXiv:astro-ph/9501045](#).
- [68] G. B. Rybicki, *Radiative Processes in Astrophysics*. Wiley-VCH, 2004.
- [69] M. S. Shaw, R. W. Romani, G. Cotter, S. E. Healey, P. F. Michelson, A. C. S. Readhead, J. L. Richards, W. Max-Moerbeck, O. G. King, and W. J. Potter, “Spectroscopy of The Largest Ever Gamma-ray Selected BL Lac Sample,” *Astrophys. J.* **764** (2013) 135, [arXiv:1301.0323 \[astro-ph.HE\]](#).
- [70] M. S. Shaw, R. W. Romani, G. Cotter, S. E. Healey, P. F. Michelson, A. C. S. Readhead, J. L. Richards, W. Max-Moerbeck, O. G. King, and W. J. Potter, “Spectroscopy of Broad Line Blazars from 1LAC,” *Astrophys. J.* **748** (2012) 49, [arXiv:1201.0999 \[astro-ph.HE\]](#).
- [71] D. Hutsemekers, B. Borguet, D. Sluse, R. Cabanac, and H. Lamy, “Optical circular polarization in quasars,” *Astron. Astrophys.* **520** (2010) L7, [arXiv:1009.4049 \[astro-ph.CO\]](#).
- [72] R. E. Pudritz, M. J. Hardcastle, and D. C. Gabuzda, “Magnetic Fields in Astrophysical Jets: From Launch to Termination,” *Space Sci. Rev.* **169** (2012) 27–72, [arXiv:1205.2073 \[astro-ph.HE\]](#).
- [73] E. Prandini and G. Ghisellini, “The Blazar Sequence and Its Physical Understanding,” *Galaxies* **10** (2022) 35, [arXiv:2202.07490 \[astro-ph.HE\]](#).
- [74] D. C. Gabuzda, E. Murray, and P. Cronin, “Helical magnetic fields associated with the relativistic jets of four bl lac objects,” *Mon. Not. Roy. Astron. Soc.* **351** (2004) L89, [arXiv:astro-ph/0405394](#).
- [75] D. C. Gabuzda, N. Roche, A. Kirwan, S. Knuettel, M. Nagle, and C. Houston, “Parsec scale Faraday-rotation structure across the jets of nine active galactic nuclei,” *Monthly Notices of the Royal Astronomical Society* **472** (08, 2017) 1–10, [arXiv:1701.00271 \[astro-ph.HE\]](#).
- [76] E. V. Kravchenko, Y. Y. Kovalev, and K. V. Sokolovsky, “Parsec-scale Faraday rotation and polarization of 20 active galactic nuclei jets,” *Mon. Not. Roy. Astron. Soc.* **467** (2017) 83–101, [arXiv:1701.00271 \[astro-ph.HE\]](#).



- [77] M. C. Begelman, R. D. Blandford, and M. J. Rees, “Theory of extragalactic radio sources,” *Rev. Mod. Phys.* **56** (1984) 255–351.
- [78] M. J. Rees, “Magnetic confinement of broad-line clouds in active galactic nuclei,” *Monthly Notices of the Royal Astronomical Society* **228** (09, 1987) 647–652.
- [79] S. P. O’Sullivan and D. C. Gabuzda, “Magnetic field strength and spectral distribution of six parsec-scale active galactic nuclei jets,” *Mon. Not. Roy. Astron. Soc.* **400** (2009) 26, [arXiv:0907.5211 \[astro-ph.CO\]](#).
- [80] A. Celotti and G. Ghisellini, “The power of blazar jets,” *Mon. Not. Roy. Astron. Soc.* **385** (2008) 283, [arXiv:0711.4112 \[astro-ph\]](#).
- [81] R. Blandford, D. Meier, and A. Readhead, “Relativistic Jets from Active Galactic Nuclei,” *Annual Review of Astronomy and Astrophysics* **57** (2019) 467–509, <https://doi.org/10.1146/annurev-astro-081817-051948>.
- [82] M. Boettcher, A. Reimer, K. Sweeney, and A. Prakash, “Leptonic and Hadronic Modeling of Fermi-Detected Blazars,” *Astrophys. J.* **768** (2013) 54, [arXiv:1304.0605 \[astro-ph.HE\]](#).
- [83] CAST Collaboration, V. Anastassopoulos *et al.*, “New CAST Limit on the Axion-Photon Interaction,” *Nature Phys.* **13** (2017) 584–590, [arXiv:1705.02290 \[hep-ex\]](#).
- [84] J. A. Grifols, E. Masso, and R. Toldra, “Gamma-rays from SN1987A due to pseudoscalar conversion,” *Phys. Rev. Lett.* **77** (1996) 2372–2375, [arXiv:astro-ph/9606028](#).
- [85] A. Payez, C. Evoli, T. Fischer, M. Giannotti, A. Mirizzi, and A. Ringwald, “Revisiting the SN1987A gamma-ray limit on ultralight axion-like particles,” *JCAP* **02** (2015) 006, [arXiv:1410.3747 \[astro-ph.HE\]](#).
- [86] M. Berg, J. P. Conlon, F. Day, N. Jennings, S. Krippendorf, A. J. Powell, and M. Rummel, “Constraints on Axion-Like Particles from X-ray Observations of NGC1275,” *Astrophys. J.* **847** (2017) 101, [arXiv:1605.01043 \[astro-ph.HE\]](#).
- [87] M. C. D. Marsh, H. R. Russell, A. C. Fabian, B. P. McNamara, P. Nulsen, and C. S. Reynolds, “A New Bound on Axion-Like Particles,” *JCAP* **12** (2017) 036, [arXiv:1703.07354 \[hep-ph\]](#).
- [88] M. Bottcher and J. Chiang, “X-Ray Spectral Variability Signatures of Flares in BL Lacertae Objects,” *The Astrophysical Journal* **581** (Dec, 2002) 127–142.
- [89] L. Maraschi and F. Tavecchio, “The jet-disk connection and blazar unification,” *Astrophys. J.* **593** (2003) 667–675, [arXiv:astro-ph/0205252](#).
- [90] F. Tavecchio, G. Ghisellini, G. Ghirlanda, L. Foschini, and L. Maraschi, “TeV BL Lac objects at the dawn of the Fermi era,” *Mon. Not. Roy. Astron. Soc.* **401** (2010) 1570, [arXiv:0909.0651 \[astro-ph.HE\]](#).
- [91] L. Valtaoja, H. Karttunen, E. Valtaoja, N. M. Shakhovskoy, and Y. S. Efimov, “Optical circular polarization in two BL Lacertae objects?,” *Astronomy and Astrophysics* **273** (June, 1993) 393–396.
- [92] S. J. Wagner and K. Mannheim, “Circular Polarization in Intraday Variable Blazars,” in *Particles and Fields in Radio Galaxies Conference*, R. A. Laing and K. M. Blundell, eds., vol. 250 of *Astronomical Society of the Pacific Conference Series*, p. 142. Jan., 2001.
- [93] L. O. Takalo and A. Sillanpää, “Simultaneous linear and circular polarization observations of blazars 3C 64A, 3C 62A and Markarian 421,” *Astrophysics and Space Science* **206** (Aug., 1993) 191–196.
- [94] Tommasi, L., Palazzi, E., Pian, E., Piirola, V., Poretti, E., Scaltriti, F., Sillanpää, A., Takalo, L., and Treves, A., “Multiband optical polarimetry of BL Lacertae objects with the Nordic Optical Telescope \*\*\*,” *A&A* **376** (2001) 51–58.
- [95] FERMI-LAT, VERITAS Collaboration, A. A. Abdo, V. A. Acciari, t. G.-W. consortium, and m.-w. partners, “Multi-wavelength Observations of the Flaring Gamma-ray Blazar 3C 66A in 2008 October,” *Astrophys. J.* **726** (2011) 43, [arXiv:1011.1053 \[astro-ph.HE\]](#). [Erratum: *Astrophys. J.* 731, 77 (2011)].
- [96] A. Reimer, M. Joshi, and M. Bottcher, “The blazar 3C 66A in 2003–2004: Hadronic versus leptonic model fits,” *AIP Conf. Proc.* **1085** (2009) 502–505.
- [97] M. P. C. Legg and K. C. Westfold, “Elliptic Polarization of Synchrotron Radiation,” *Astrophys. J.* **154** (Nov., 1968) 499.
- [98] D. B. Melrose, “On the Degree of Circular Polarization of Synchrotron Radiation,” *Astrophysics and Space Science* **12** (July, 1971) 172–192.
- [99] I. Liodakis, D. Blinov, S. B. Potter, and F. M. Rieger, “Constraints on magnetic field and particle content in blazar jets through optical circular polarization,” *Mon. Not. Roy. Astron. Soc.* **509** (2021) L21–L25, [arXiv:2110.11434 \[astro-ph.HE\]](#).
- [100] F. Govoni and L. Feretti, “Magnetic field in clusters of galaxies,” *Int. J. Mod. Phys. D* **13** (2004) 1549–1594, [arXiv:astro-ph/0410182](#).
- [101] L. Feretti, G. Giovannini, F. Govoni, and M. Murgia, “Clusters of galaxies: observational properties of the diffuse radio emission,” *Astron. Astrophys. Rev.* **20** (2012) 54, [arXiv:1205.1919 \[astro-ph.CO\]](#).
- [102] P. Blasi, S. Burles, and A. V. Olinto, “Cosmological magnetic fields limits in an inhomogeneous universe,” *Astrophys. J. Lett.* **514** (1999) L79–L82, [arXiv:astro-ph/9812487](#).
- [103] A. De Angelis, M. Persic, and M. Roncadelli, “Constraints on Large-Scale Magnetic Fields from the Auger Results,” *Mod. Phys. Lett. A* **23** (2008) 315–317, [arXiv:0711.3346 \[astro-ph\]](#).
- [104] Pierre Auger Collaboration, P. Abreu *et al.*, “Update on the Correlation of the Highest Energy Cosmic Rays with Nearby Extragalactic matter,” *Astropart. Phys.* **34** (2010) 314–326, [arXiv:1009.1855 \[astro-ph.HE\]](#).
- [105] WMAP Collaboration, G. Hinshaw *et al.*, “Nine-Year Wilkinson Microwave Anisotropy Probe (WMAP) Observations: Cosmological Parameter Results,” *Astrophys. J. Suppl.* **208** (2013) 19, [arXiv:1212.5226 \[astro-ph.CO\]](#).
- [106] R. Jansson and G. R. Farrar, “A New Model of the Galactic Magnetic Field,” *Astrophys. J.* **757** (2012) 14, [arXiv:1204.3662 \[astro-ph.GA\]](#).
- [107] R. Jansson and G. R. Farrar, “The Galactic Magnetic

- Field,” *Astrophys. J. Lett.* **761** (2012) L11, [arXiv:1210.7820 \[astro-ph.GA\]](#).
- [108] K. Dolag, D. Grasso, V. Springel, and I. Tkachev, “Constrained simulations of the magnetic field in the local Universe and the propagation of UHECRs,” *JCAP* **01** (2005) 009, [arXiv:astro-ph/0410419](#).
- [109] J. N. Bregman, R. A. Dupke, and E. D. Miller, “Cosmic filaments in superclusters,” *Astrophys. J.* **614** (2004) 31–36, [arXiv:astro-ph/0407365](#).
- [110] I. Suhhonenko, J. Einasto, L. J. Liivamägi, E. Saar, M. Einasto, G. Hutsi, V. Muller, A. A. Starobinsky, E. Tago, and E. Tempel, “The cosmic web for density perturbations of various scales,” *Astron. Astrophys.* **531** (2011) A149, [arXiv:1101.0123 \[astro-ph.CO\]](#).
- [111] M. Einasto, H. Lietzen, E. Tempel, M. Gramann, L. J. Liivamägi, and J. Einasto, “SDSS superclusters: morphology and galaxy content,” *Astron. Astrophys.* **562** (2014) A87, [arXiv:1401.3226 \[astro-ph.CO\]](#).
- [112] R. B. Tully, H. Courtois, Y. Hoffman, and D. Pomarède, “The Laniakea supercluster of galaxies,” *Nature* **513** (2014) 71, [arXiv:1409.0880 \[astro-ph.CO\]](#).
- [113] M. Einasto, B. Deshev, P. Tenjes, P. Heinämäki, E. Tempel, L. J. Liivamägi, J. Einasto, H. Lietzen, T. Tuvikene, and G. Chon, “Multiscale cosmic web detachments, connectivity, and preprocessing in the supercluster SC1A2142 cocoon,” *Astron. Astrophys.* **641** (2020) A172, [arXiv:2007.04910 \[astro-ph.CO\]](#).
- [114] K. Dolag, D. Grasso, V. Springel, and I. Trachev, “Simulating the Magnetic Field in the Local Supercluster,” in *X-Ray and Radio Connections*, L. O. Sjouwerman and K. K. Dyer, eds., p. 8.10. Apr., 2005.
- [115] F. Vazza, C. Ferrari, M. Brüggen, A. Bonafede, C. Gheller, and P. Wang, “Forecasts for the detection of the magnetised cosmic web from cosmological simulations,” *Astron. Astrophys.* **580** (2015) A119, [arXiv:1503.08983 \[astro-ph.CO\]](#).
- [116] F. Vazza *et al.*, “Magnetogenesis and the Cosmic Web: A Joint Challenge for Radio Observations and Numerical Simulations,” *Galaxies* **9** (2021) 109, [arXiv:2111.09129 \[astro-ph.CO\]](#).
- [117] M. S. S. L. Oei, R. J. van Weeren, F. Vazza, F. Leclercq, A. Gopinath, and H. J. A. Röttgering, “Filamentary baryons and where to find them - A forecast of synchrotron radiation from merger and accretion shocks in the local Cosmic Web,” *Astron. Astrophys.* **662** (2022) A87, [arXiv:2203.05365 \[astro-ph.CO\]](#).